Thickness Dependence of Structural and Optical Properties of CdTe Films

R. Zarei Moghadam, M. H. Ehsani*, H. Rezagholipour Dizaji and M. R. Sazideh

* *ehsani@semnan.ac.ir*

Received: January 2018 **Accepted: June 2018**

Faculty of Physics, Semnan University, Semnan, Iran.

DOI: 10.22068/ijmse.15.3.21

Abstract: *In this work, Cadmium Telluride (CdTe) thin films were deposited on glass substrates at room temperature by vacuum evaporation technique. The deposited CdTe thin films were characterized by X-ray diffraction, UV-Visible spectroscopy, and Field emission scanning electron microscopy (FESEM) techniques. Structural studies revealed that the CdTe films deposited at various thicknesses were crystallized in a cubic structure. The results showed improvement of the film crystallinity upon grain size increment. Optical constants such as refractive index (n), extinction coefficient (k), real and imaginary parts of dielectric constant, volume energy loss function (VELF), and surface energy loss function (SELF) were calculated using data provided by UV-Vis spectra. In addition, band gap and Urbach energies were calculated by Tauc and ASF methods. The band gap energy of the specimens was found to decrease from 1.8 to 1.4eV with increasing the thickness of films. The absorption coefficient; computed and plotted versus photon energy (hv), and tailing in the optical band gap was observed which was understood based on Urbach law. Urbach energy variation from 0.125 to 0.620 eV in the samples with higher thicknesses is concluded.*

Keywords: *Cadmium Telluride (CdTe), Thin films, Evaporation technique, Urbach energy.*

1. INTRODUCTION

The study of II–VI binary semiconductor compounds have been exacerbated in order to find new applications, mainly in solar cells [1, 2]. Cadmium telluride has been recognized as one of the most promising II–VI compound semiconductors for manufacturing solar cell films [3, 4, 5]. Because of its optimum energy band gap (1.44eV) at room temperature and high absorption coefficient (>10+5cm-1) in the visible region, CdTe can act as a good candidate for solar energy conversion [6, 7]. Furthermore, this material has other applications, particularly in the field of optoelectronic devices like gamma and X-ray detectors [8], light emitting diodes (LEDs) [9], field effect transistors (FETs) [10], lasers [11], nonlinear integrated optical devices [1] etc.

CdTe thin films can be fabricated by various methods such as sputtering [12], electro deposition [13], pulsed laser deposition (PLD) [14], spray pyrolysis [15], thermal evaporation [16], metal organic chemical vapor deposition (MOCVD) [17], chemical bath deposition (CBD) [18], molecular beam epitaxy (MBE) [19], successive ionic layer adsorption and reaction [20, 21] etc.

Thermal vacuum evaporation is one of the most applicable and proper methods to produce CdTe thin films because of its various advantages such as high deposition rate, low material consumption and low cost of operation. The physical and chemical properties of thin films are highly dependent on the preparation technique, film thickness, annealing and substrate temperature [1]. Several experiments have been already reported on optical and electrical properties of CdTe films [22- 25]. Nasser and his co-workers prepared CdTe thin films by physical vapor deposition and investigated their structural and optical properties such as Urbach tails and observed the Urbach tails increment with increasing film thickness [29]. Punitha et al., have studied the annealing impressions on optical properties and surface morphology of CdTe films [24]. Hu et al., have investigated the influence of substrate temperature on the properties of PLD prepared CdTe thin films [30].

In the present investigation, CdTe thin films with different thicknesses were deposited on glass substrates using thermal vacuum evaporation method at room temperature. The main idea behind the present study is to investigate the influence of CdTe film thickness

[DOI: 10.22068/ijmse.15.3.21]

on its structural and optical properties. Also, for calculating band gap energy and Urbach tail, two methods, namely; Tauc and absorption spectrum fitting (ASF) were used and the results obtained from both the methods have been compared. The advantage of ASF method in comparison with the Tauc method lies in its ability to estimate band gap of the film with no need to know the kind of transition (direct or indirect) and film thickness.

2. EXPERIMENTAL DETAILS

CdTe thin films were deposited onto glass substrates by thermal evaporation technique in Hind-HIVC coating unit (Model 15F6) under a chamber work pressure of 5×10^{-5} mbar at room temperature. Prior to the deposition process, the glass substrates were cleaned in acetone and deionized water using the ultrasonic bath for 14 min and dried by purified nitrogen gas. CdTe powder of 99.99% purity, supplied by Aldrich Company, was evaporated within a molybdenum boat. The distance between source and substrate was fixed at 19 cm. The average rate of deposition was 10 Å/s. Four CdTe thin films with various thicknesses (100, 200, 400, and 600 nm) were produced and labeled as S_1, S_2, S_3, and S_4, respectively.

The thickness of CdTe thin films evaluated by Scanning Electron Microscope (SEM) (VEGA\\TESCAN - XMU). The crystal structure of the prepared samples was analyzed using X-ray diffraction spectrometer (ADVANCE–D8 model) equipped with Cu k_α radiation source with λ= 1.5406Å, the voltage of 40 kV, and electron current of 40 mA. The optical properties such as extinction coefficient (k), refractive index(n), band gap (E_g), the Urbach tail (E_u), dielectric constants, energy loss function of CdTe thin films were studied by UV-visible spectrophotometer (PerkinElmer model Lambda-25) in the wavelength range of 300 nm-1100 nm.

3. RESULTS AND DISCUSSIONS

3. 1. Thickness Analysis

Fig. 1 shows the FESEM cross-section micrographs of the prepared samples. The thickness of samples, calculated by Digimizer software using their cross-section images, was found to be 197.27 nm, 300 nm, 536.07 nm, and 846.43 nm for S_1, S_2, S_3, and S_4 samples, respectively.

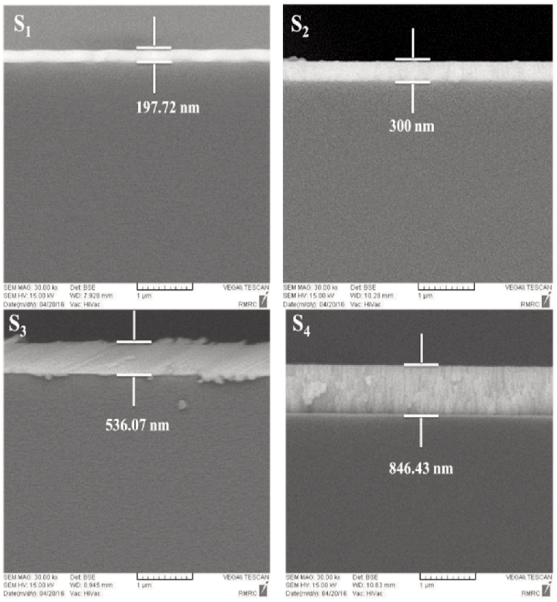

Fig. 1. FESEM cross- section images of S_1, S_2, S_3, and S_4 samples.

3. 2. Structural Properties

The X-ray diffraction patterns of CdTe films of various thicknesses presented in Fig. 2. The diffraction peaks observed at 2θ=23.7, 39.31, and 46.43 degrees are, respectively, corresponding to (111), (220) and (311) crystallographic planes which are confirmed by the JCPDS data file (#00-015- 0770) with cubic phase structure. This figure also shows the peak intensity increment upon increasing the film thickness which is an indication of films crystallinity improvement due to film thickness increment. For the peak related to (111) plane, crystallite size (D) of samples is calculated using Debye – Scherrer formula [1]:

$$D=\frac{0.9\lambda}{\beta\cos\theta} \quad (1)$$

Here θ is the diffraction angle, λ is the X-ray wavelength (λ= 1.5406Å), β is the width of the peak at half maximum intensity. The average D value

[DOI: 10.22068/ijmse.15.3.21]

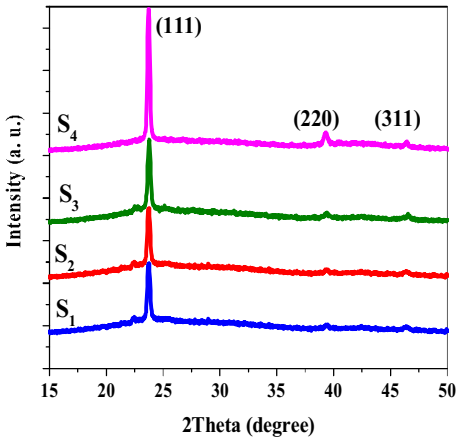

Fig. 2. The X-ray diffraction patterns of S_1, S_2, S_3, and S_4 samples.

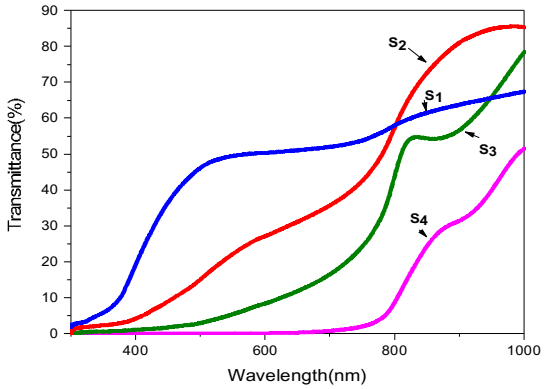

Fig. 3. Transmittance spectra of S1, S2, S3, and S4 samples.

calculated for S_1, S_2, S_3, and S_4 specimens was found to be 25.9, 29.4, 29.7 and 34.4 nm, respectively. The crystallinity improvement of CdTe films through increasing the thickness has been reported by others [22, 25-28]. Wu et al. reported the crystallite size increment from 24 to 31 nm, as the thickness increased from 0.3 to 1.2 μm [31].

3. 3. Optical Properties

3. 3. 1. Optical Transmittance and Band Gap Energy

Usually, the deposition conditions affect the optical properties of thin films. Fig. 3 shows the transmittance spectra of S_1, S_2, S_3, and S_4 specimens obtained in the wavelength range of 300 nm to 1100 nm. All the samples show low transmission in the visible region except for S1 which has the relatively high transmission. In fact, the average transmittance of the films decreased with increasing film thickness. By increasing the thickness of the films, the structure becomes denser, more regular and porosity was decreased therefor average transmittance was decreased By increasing the thickness and the grain size, the light passes through the layer was trapped between the structure. Therefore, it decreases with increasing optical transducer thickness. In addition, it is concluded that the absorption edges shift towards longer wavelength regions, indicates a systematic decrease in the band gap energy with increasing thickness of thin film [32].

The absorption coefficient (α) of films, calculated from the equation α=Ln(1/T)/t (where T is transmittance and t is the thickness of layers), was found to be in the range of 10^4 -10^5 cm^{-1}. The band gap energy of the specimens was calculated using Tauc relation [33]:

$$\alpha h\nu = A(h\nu - E_g)^N \quad (2)$$

where α is the absorption coefficient, E_g is the band gap energy, hυ is the photon energy, and A is a constant depending on the material refractive index and the effective masses of electron and hole. N value equals 1/2 and 2 for the direct and indirect transition materials, respectively [34-36]. The graph of $(\alpha h\nu)^2$ versus photon energy is illustrated in Fig. 4. The band gap energy values are obtained by extrapolating the linear portion of the curves to the x-axis.

It is observed from Fig. 4 that the bandgap energy of the specimens decreases upon increasing the film thickness. The direct evaluate Both values of band gap energies for each samples for S_1, S_2, S_3, and S_4 samples are estimated by using the Tauc method as (1.43, 1.85 eV), (1.41, 1.54 eV), (1.24, 1.5 eV), and (1.22, 1.38 eV), respectively, exhibiting a reverse relation of band gap energy with film thickness. The obtained E_g values are consistent with the results reported by Chopra et al. [34]. They

[DOI: 10.22068/ijmse.15.3.21]

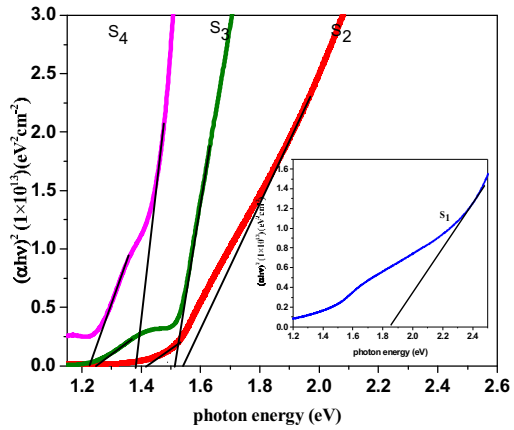

Fig. 4. Graph of versus photon energy for all the samples.

observed the direct band gap of RF-sputtered CdTe films in the range of (1.41–1.5 eV) with various RF powers and vacuum levels. Turky and Dawy [35], reported the film thickness-induced variation in energy band gap (1.45–1.5 eV) of thermally evaporated CdTe thin films. Also, Chander and Dhaka [25] reported the effect of thickness on energy band gap (1.4-1.6 eV) of thermally evaporated CdTe thin films [25].

The results show that by increasing the samples thickness, crystallinity increases. This is due to the increment in crystallite size resulting in band gap reduction. The obtained values are in good agreement with the results of the structural analysis. Crystallinity improvement by increasing the thickness of the CdTe films has also been reported by others [22, 25].

Despite Tauc method, a new method of absorption spectrum fitting (ASF) was used for estimating the band gap energy. This method, unlike Tauc method, doesn't need thickness value of a layer for determining its band gap energy. The ASF method uses Beer-Lambert law in the form of $\alpha(\lambda) = B(h)^{m-1}$, where α is absorption coefficient calculated from the following equation:

$$\alpha(\lambda) = 2.303A/z \quad (3)$$

z and A are the film thickness and layer absorption, respectively. m can be one of these values: 0.5, 1.5, or 2.3 [34- 36]. In ASF method, the band gap energy can be calculated by the following equation:

$$E_{gap}^{ASF} = hc/\lambda_g = 1239.83/\lambda_g \quad (4)$$

Here h is the Planck constant, c is the speed of light, and λ_g is the wavelength of the corresponding band gap energy. Using Beer-Lambert law, one can calculate absorption coefficient as follows [24, 29, 30, 37]:

$$A(\lambda) = D\lambda(1/\lambda - 1/\lambda g)^m \quad (5)$$

where $D=[B(hc)^{m-1}]$.

Fig. 5 demonstrates the absorption spectra of S_1, S_2, S_3, and S_4 samples obtained in the wavelength range from 300 nm to 1100 nm.

The results show that by increasing the thickness of the thin films, the absorption increases. The data obtained from $(A/\lambda)^2$ curve versus $(1/\lambda)$ are used for estimating band gap energy employing ASF method (Fig. 6). Using the linear part of a curve, $(1/\lambda_g)$ can be calculated which is then used to estimate its band gap energy by $E_{gap}^{ASF} = 1239.83/\lambda_g$ relation. Values of band gap energy for S_1, S_2, S_3 and S_4 samples are estimated to be 1.897 eV, 1.884 eV, 1.698 eV, and 1.537 eV, respectively, using ASF method. The

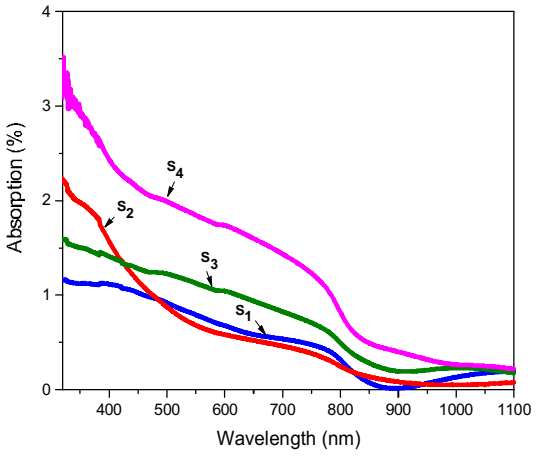

Fig. 5. Absorption spectra of S_1, S_2, S_3, and S_4 samples.

[DOI: 10.22068/ijmse.15.3.21]

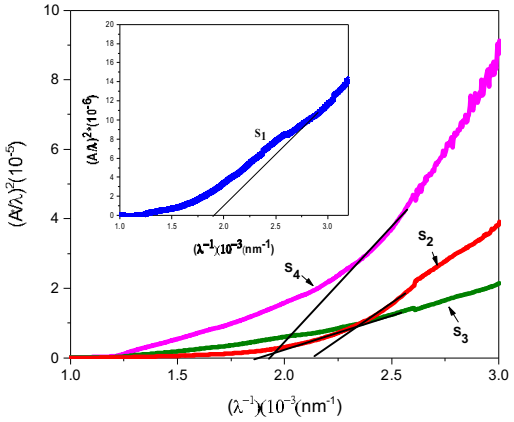

Fig. 6. ASF plot for the evaluation of band gap of S_1, S_2, S_3, and S_4 samples.

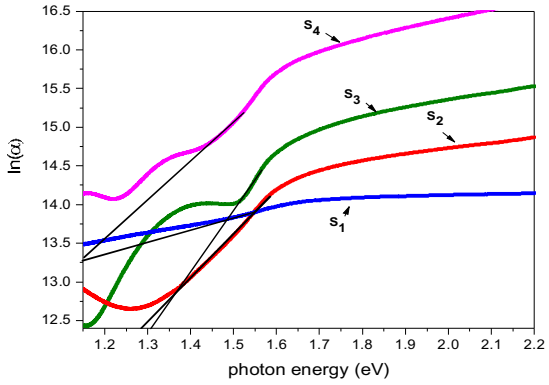

Fig. 7. Ln(α) versus photon energy for S_1, S_2, S_3, and S_4 samples.

results show that increasing the film thickness from 200 nm to 850 nm, has led to decreasing the band gap, in addition to the improving the film crystallinity. others [25] have reported the effect of increasing the thickness of a film on improving its crystallinity. Also, values of band gap energy obtained by ASF method are given in Table 1.

3. 3. 2. Urbach Tails and Disorder

Urbach energy (E_{tail}) is the tail width of localized states corresponding to the optical shift between localized tail states adjacent to valence band and an extended state in the conduction band lying above the mobile edge. It may be formed as a result of grain boundaries, surface dangling bonds, vacancies, defects, imperfections, excitonics, and interstitials [38]. The Urbach energy can be investigated as a function of temperature and structural disorders. In the present study, both the Tauc and the new ASF methods have been used to calculate the Urbach energy and finally, the results have been compared. The Tauc method described by the following formula shows the photon energy dependence of absorption coefficient.

$$\alpha = \alpha_0 \, exp(h\nu/E_u) \qquad (6)$$

Here α_0 and E_u are constants determined by fitting the experimental data [39, 40]. Fig. 7, represents the ln(α) versus photon energy for S_1, S_2, S_3, and S_4 samples. Urbach energy was calculated from the slope of the linear portion of the related curve of each sample. Using Tauc method, Urbach energy is attained to be 0.620, 0.171, 0.127, and 0.125 eV for S_1, S_2, S_3, and S_4 samples, respectively. Therefore, the results prove the reduction in Urbach energy and disorder upon increment in the thickness of the specimens. The obtained Urbach energy results of all the samples using Tauc method are provided in Table 1.

In ASF method, the exponential law is given as below:

$$A(\lambda) = D_1 exp(h\nu/E_{Tail}\lambda) \qquad (7)$$

where D_1 is constant, and E_{Tail} is the tail width of the localized states. The value of E_{tail} can be estimated from the slope of the linear portion of the ln(A) versus (λ^{-1}) curve by using the E=1239.83/slope relation. The graph of ln(A) versus (λ^{-1}) for S_1, S_2, S_3 and S_4 samples are represented in Fig. 8. Using ASF method and the data provided by this figure, the Urbach energy for S_2, S_3 and S_4 samples was estimated and the results have been presented in Table 1.

It can be inferred from Table 1 that Urbach and band gap energy values decrease with increasing the thickness of layers from 200 nm to 850 nm, indicating the improvement of the film crystallinity due to the reduction of structural defects [29]. Fig. 9, provides a comparison

[DOI: 10.22068/ijmse.15.3.21]

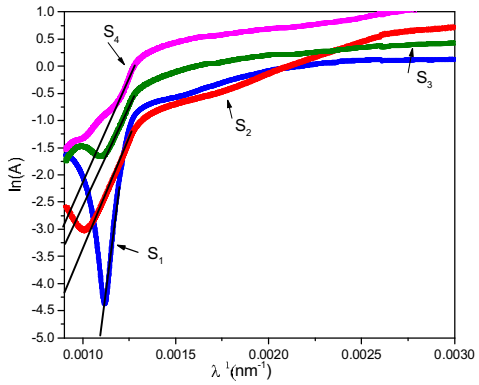

Fig. 8. The graph of ln(A) versus (-1) for S_1, S_2, S_3, and S_4 samples.

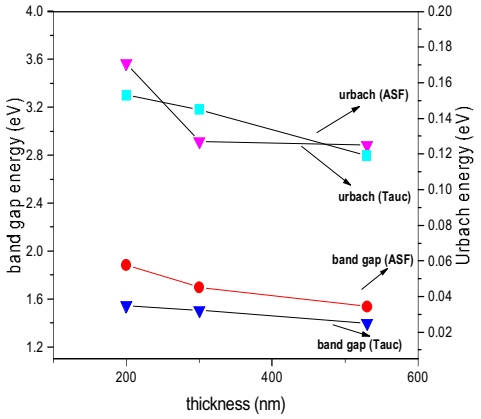

Fig. 9. Comparison among the values of Urbach energy and band gap of S_2, S_3, and S_4 samples estimated by Tauc and ASF methods.

among the values of the Urbach energy and band gap of S_2, S_3 and S_4 samples estimated by Tauc and ASF methods. As one can see in Table 1 and Fig. 9, the Urbach tail and band gap energy dependence on thickness, follow a specific order. In addition, a good agreement is also observed between the results obtained from the Tauc and ASF methods.

3. 3. 3. Optical Constants

When passing through some materials, an electromagnetic wave may lose some amount of its energy in such a way that N (=light refractive index in the dielectric or lighting environment) is divided into two parts. One of them is imaginary which is nominated extinction coefficient (K), and the other is real that is called refractive index (n). The extinction coefficient is known to provide information about the absorption of light in the medium material due to inelastic scattering [24] and is given by $K = \alpha\lambda/(4\pi)$. Here α is the absorption coefficient of the material. Figure 10a demonstrates the extinction coefficient of S_1, S_2, S_3 and S_4 samples. The figure shows that at the wavelength of 1050 nm, the extinction coefficient of the films increases upon increasing their thickness. By increasing the thickness of CdTe thin films from 200 nm to 850 nm, the extinction coefficient gets increased from 0.062 to 0.115 at 1050 nm wavelength.

One of the most fundamental characteristics of the optical properties is optical refractive index because of its proximate relation with the electronic polarizability of ions and local field, located in the materials [24]. This parameter can be utilized to compute the electronic polarizability of a material. The refractive index can be calculated by many methods such as Swanepoel and Sellinp [41]. In this study, Swanepoel method is used for calculating the refractive index of CdTe thin films taking the following formula into account:

Table 1. Optical parameters of S_1, S_2, S_3, and S_4 samples.

samples	S_1=200	S2=300	S3=550	S_4=850
E_g(eV) (Tauc)	1.834, 1.43	1.545, 1.41	1.506, 1.24	1.4, 1.22
E_g(eV) (ASF)	1.897	1.884	1.698	1.537
E_u(eV) (Tauc)	0.62	0.171	0.127	0.125
E_u(eV) (ASF)	-	0.153	0.145	0.119
n	3.55	2.11	2.76	5.54
k	0.062	0.031	0.02	0.115
ε_1	12.45	5.82	4.35	33.05
ε_2	0452	0.232	0.158	1.33

[DOI: 10.22068/ijmse.15.3.21]

$$n = \frac{1+R}{1-R} + \sqrt{\frac{4R}{(1-R)^2} - K^2} \quad (8)$$

where R is reflection coefficient and k is extinction coefficient [37, 42, 43]. Fig. 10b shows the refractive index of S_1, S_2, S_3 and S_4 samples versus wavelength. This figure illustrates that in the wavelength of 1050 nm, the refractive index of the films increases upon increasing their thickness. This may be attributed to the crystallinity improvement of the films, leading to decrement of their structural disorder. Using Eq. 8, the refractive index values of S_1, S_2, S_3 and S_4 samples were calculated at 1050 nm wavelength and found to be 3.55, 2.4, 2.76, and 5.54 for, respectively. The refractive indices and extinction coefficients of the specimens have been presented in Table 1. Punitha et al. obtained the refractive index in the range of 2.46 to 2.52 and extinction coefficient in the range of 0.03 to 0.07 for electron beam evaporated CdTe thin films, which match well with our results [24]. On the other hand, El-shazly and H. El-Shair [44], have reported the refractive index change between 2.70 and 3.10, despite extinction coefficient variation between 0 and 0.5. This wide difference may be ascribed to the structural significance of the films.

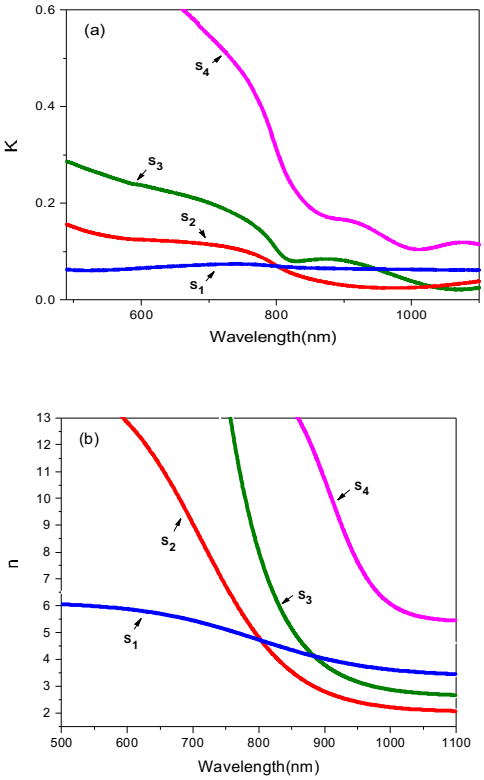

Fig. 10. (a) Extinction coefficient, and (b) refractive index of S_1, S_2, S_3, and S_4 samples.

3. 4. Dielectric properties

3. 4. 1. Dielectric Constants

It is well-known that the dielectric constant (ε) of a material is its intrinsic property, which is highly dependent on its electronic structure. It has a direct relationship with the density of states inside the band gap that affects the electromagnetic radiations passing through the material. ε is given by the following formula:

$$\varepsilon = \varepsilon_1 + i\varepsilon_2 \quad (9)$$

where ε_1 and ε_2 are real and imaginary parts, respectively [45]. The real part of a dielectric constant given by is related to the speed of the light in the material. The imaginary part given by $\varepsilon_2=2nk$ provides the situation for absorbing the energy of the electric field. ε_1 and ε_2 variations with wavelength for S_1, S_2, S_3 and S_4 samples are shown in Fig. 11. This figure shows the increment of and with film thickness increment. An inverse relation between dielectric constant and film thickness is obviously observed from the figure.

3. 4. 2. Energy Loss Function

Inelastic scattering process of electrons on a surface can be introduced by energy loss function in dielectric function [46]. The energy loss is related to the optical properties of the material via a dielectric function. The volume and surface loss functions are functions of photon energy when fast electrons passing through the bulk and surface of a material [47]. Volume energy loss function (VELF) and surface energy loss function (SELF) are dependent on real and imaginary

[DOI: 10.22068/ijmse.15.3.21]

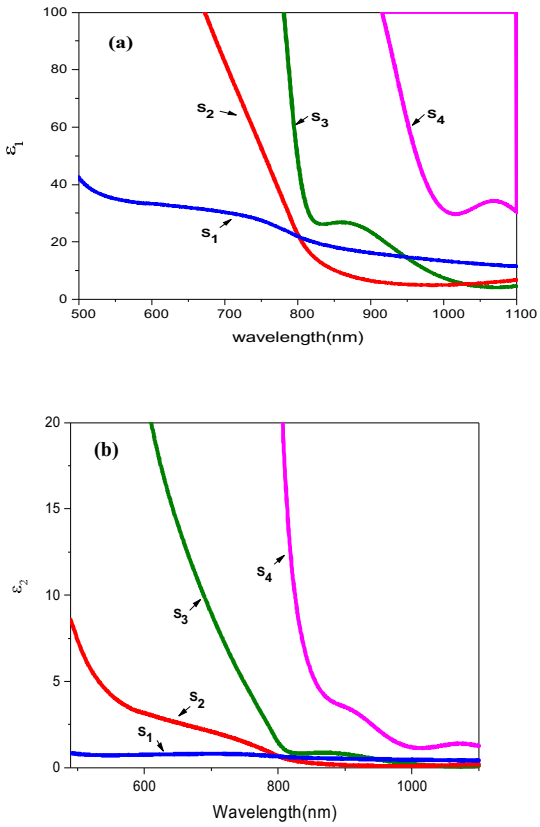

Fig. 11. (a) real and (b) imaginary parts of dielectric constant for S_1, S_2, S_3, and S_4 samples.

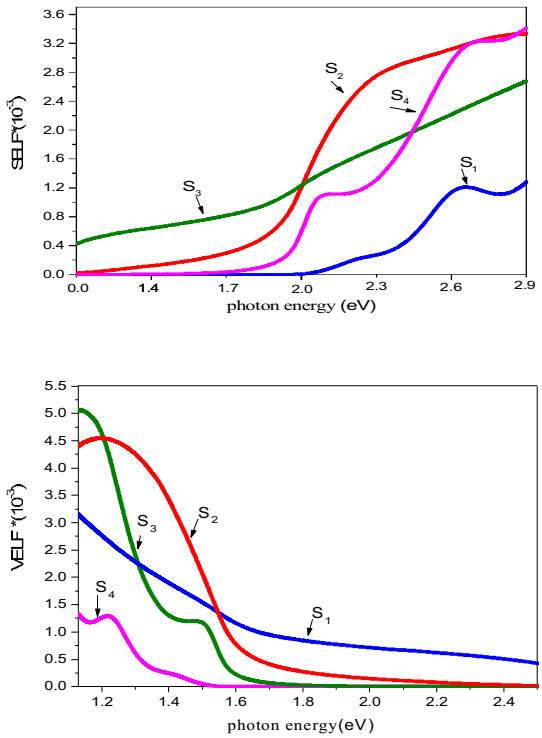

Fig. 12. VELF and SELF versus photon energy of S_1, S_2, S_3, and S_4 samples.

parts of dielectric functions, which can be calculated by $VELF=\varepsilon_2/(\varepsilon_1^2+\varepsilon_2^2)$ and $SELF=\varepsilon_2/((\varepsilon_1+1)^2+\varepsilon_2^2)$ equations [48].

The energy loss by the free charge carriers when traversing through the bulk material has fairly the same behavior as when they traverse the surface [24]. The changes in VELF and SELF versus photon energy of CdTe thin films, deposited at different thicknesses, are demonstrated in Fig. 12. The graphs presented in this figure show the difference between SELF and VELF changes with photon energy for film thicknesses from 200 nm to 850nm. With the increase in thickness of the specimens, both the VELF and SELF values decrease and thus, result in the decrease of electron energy loss. These losses are having nearly identical behavior and mainly due to the free charge carriers those travelled through the surface and volume. Also inelastic scattering process of electrons on a surface can be introduced by energy loss function in dielectric function. Obviously, the volume energy loss is greater than surface energy loss at a given incident photon energy. It is also clear that the minima of SELF and VELF correspond to the absorption energy due to the interband transition occurring at 324 nm. As one can see in Fig. 12, the maximum values of SELF and VELF nearly occur around the band gap energy then achieve the maximum energy.

4. CONCLUSIONS

In this paper, Cadmium Telluride (CdTe) thin films of different thicknesses were deposited on glass substrates at room temperature by vacuum evaporation method. Field emission scanning electron microscope (FESEM) revealed the thickness of the prepared samples. The X-ray diffraction patterns of the specimens revealed that the films were crystallized in cubic structure with the preferred orientation of (111)

[DOI: 10.22068/ijmse.15.3.21]

crystallographic plane. It was observed that the crystallites size increased with increasing the film thickness. The optical constants like refractive index (n), extinction coefficient (k), real and imaginary parts of dielectric constant, volume energy loss function (VELF), and surface energy loss function (SELF) were calculated by using UV spectra of the samples. The band gap energy was found to vary from 1.834 to 1.4 eV for thinnest (200 nm) to thickest (850 nm) prepared films, respectively, showing a reverse relation between the band gap energy of the specimens and their thickness. The results indicate that the optical properties can be improved by increasing the thickness of the CdTe thin films.

REFERENCES

1. Chander, S. and Dhaka, M., "Optimization of physical properties of vacuum evaporated CdTe thin films with the application of thermal treatment for solar cells". Mater. Sci. Semicond. Process., 2015, 40, 708-712.
2. Moghadam, R. Z., Ahmadvand, H. and Jannesari, M., "Design and fabrication of multi-layers infrared antireflection coating consisting of ZnS and Ge on ZnS substrate". Infrared Phys. Technol., 2016, 75, 18-21.
3. Chopra K. and Das S. R., "Thin Solar Cells". Plenum Press New York., USA, 1983.
4. Ismail, B. and Gould, R., "Structural and electronic properties of evaporated thin films of cadmium telluride". Phys. Status Solidi A., 1989, 115, 237-245.
5. Chander, S. and Dhaka, M. S. "Thermal evolution of physical properties of vacuum evaporated polycrystalline CdTe thin films for solar cells." J Mater Sci: Mater Electron., 2016, 27, 11961-11973.
6. Chander, S. and Dhaka, M., "Impact of thermal annealing on physical properties of vacuum evaporated polycrystalline CdTe thin films for solar cell applications". Physica E., 2016, 80, 62-68.
7. Chander S. and Dhaka M. S. "Time evolution to CdCl2 treatment on Cd-based solar cell devices fabricated by vapor evaporation." Sol Energ., 2017, 150, 577-583.
8. Goldsmid H., Giutronich J. and Kaila M., "Impact of thermal annealing on physical properties of vacuum evaporated polycrystalline CdTe thin films for solar cell applications". SOL ENERGY., 1980, 24, 435-440.
9. Gunjal, S., Khollam, Y., Jadkar, S., Shripathi, T., Sathe, V., Shelke, P., Takwale, M. and Mohite, K., "Spray pyrolysis deposition of p-CdTe films: Structural, optical and electrical properties". SOL ENERGY., 2014, 106, 56-62.
10. Rizzo, A., Li, Y., Kudera, S., Della Sala, F., Zanella, M., Parak, W. J., Cingolani, R., Manna, L. and Gigli, G., "Blue light emitting diodes based on fluorescent Cd Se⁄Zn S nanocrystals". Appl. Phys. Lett., 2007, 90, 051106-051109.
11. Wu, B., Kuo, L., DePuydt, J., Haugen, G., Haase, M. and Salamanca Riba, L., "Growth and characterization of II–VI blue light emitting diodes using short period superlattices". Appl. Phys. Lett., 1996, 68, 379-381.
12. Islam, M., Huda, Q., Hossain, M., Aliyu, M., Karim, M., Sopian, K. and Amin, N., "High quality 1 μm thick CdTe absorber layers grown by magnetron sputtering for solar cell application" Curr. Appl. Phys., 2013, 13, 115-121.
13. Echendu, O., Fauzi, F., Weerasinghe, A. and Dharmadasa, I., "High short-circuit current density CdTe solar cells using all-electrodeposited semiconductors". Thin Solid Films., 2014, 556, 529-534.
14. Ghosh, B., Hussain, S., Ghosh, D., Bhar, R. and Pal, A., "Studies on CdTe films deposited by pulsed laser deposition technique". Physica B: Condensed Matter., 2012, 407, 4214-4220.
15. Nikale, V., Shinde, S., Bhosale, C. and Rajpure, K., "Physical properties of spray deposited CdTe thin films: PEC performance". J. Semicond., 2011, 32, 033001-033008.
16. Khairnar, U., Bhavsar, D., Vaidya, R. and Bhavsar, G., "Optical properties of thermally evaporated cadmium telluride thin films". Mater. Chem. Phys., 2003, 80, 421-427.
17. Zoppi, G., Durose, K., Irvine, S. and Barrioz, V., "Grain and crystal texture properties of absorber layers in MOCVD-grown CdTe/CdS solar cells". Semicond. Sci. Technol., 2006, 21, 763-770.
18. Dhanam, M., Prabhu, R. R. and Manoj, P.,

[DOI: 10.22068/ijmse.15.3.21]

"Investigations on chemical bath deposited cadmium selenide thin films". Mater. Chem. Phys., 2008, 107, 289-296.
19. Oehling, S., Lugauer, H., Schmitt, M., Heinke, H., Zehnder, U., Waag, A., Becker, C. and Landwehr, G., "p type doping of CdTe with a nitrogen plasma source". J. Appl. Phys., 1996, 79, 2343-2346.
20. Ubale, A., Dhokne, R., Chikhlikar, P., Sangawar, V., Kulkarni, D., "Characterization of nanocrystalline cadmium telluride thin films grown by successive ionic layer adsorption and reaction (SILAR) method". Bull. Mater. Sci., 2006, 29, 165-168.
21. Romeo, A., Bätzner, D., Zogg, H., Vignali, C. and Tiwari, A., "Influence of CdS growth process on structural and photovoltaic properties of CdTe/CdS solar cells". Sol. Energy Mater. Sol. Cells., 2001, 67, 311-321.
22. Shaaban, E., Afify, N. El-Taher, A., "Effect of film thickness on microstructure parameters and optical constants of CdTe thin films". J. Alloys Compd., 2009, 482, 400-404.
23. Dongol, M., El-Denglawey, A., El Sadek, M. A. and Yahia, I., "Thermal annealing effect on the structural and the optical properties of Nano CdTe films". Optik., 2015, 126, 1352-1357.
24. Punitha, K., Sivakumar, R., Sanjeeviraja, C. and Ganesan, V., "Influence of post-deposition heat treatment on optical properties derived from UV–vis of cadmium telluride (CdTe) thin films deposited on amorphous substrate". Appl. Surf. Sci., 2015, 344, 89-100.
25. Chander, S. and Dhaka, M., "Influence of thickness on physical properties of vacuum evaporated polycrystalline CdTe thin films for solar cell applications". Physica E., 2016, 76, 52-59.
26. Prathap, P., et al. "Thickness effect on the microstructure, morphology and optoelectronic properties of ZnS films." Journal of Physics: Condensed Matter 20.3 (2007): 035205.
27. Nakamura, Kyotaro, "Influence of CdS window layer on 2-μm thick CdS/CdTe thin film solar cells." Solar energy materials and solar cells 75.1-2 (2003): 185-192.
28. Ubale, A. U., and D. K. Kulkarni. "Preparation and study of thickness dependent electrical characteristics of zinc sulfide thin films." Bulletin of Materials Science 28.1 (2005): 43-47.
29. Nassar Z. M., Yükselici M. H. and Bozkurt A. A., "Structural and optical properties of CdTe thin film: A detailed investigation using optical absorption, XRD, and Raman spectroscopies". Phys. Status Solidi B., 2016, 253, 1104–1114.
30. Hu, P., Li, B., Feng, L., Wu, J., Jiang, H., Yang, H. and Xiao, X., "Effects of the substrate temperature on the properties of CdTe thin films deposited by pulsed laser deposition" Surf. Coat. Technol., 2012, 213, 84-89.
31. Wu, X., Lai, F., Lin, L., Lv, J., Zhuang, B., Yan, Q. and Huang, Z., "Optical inhomogeneity of ZnS films deposited by thermal evaporation". Appl. Surf. Sci., 2008, 254, 6455–6460.
32. Kim, N. H., Park, C. I. and Lee, H. Y., "Microstructure, stress and optical properties of CdTe thin films laser-annealed by using an 808-nm diode laser: Effect of the laser scanning velocity". J. Korean Phys. So., 2013, 63, 229-235.
33. Larbi, A., Dahman, H. and Kanzari, M., "Effect of substrate temperature on structural and optical properties of the new high absorbent Sn 3 Sb 2 S 6 thin films". Vacuum., 2014, 110, 34-39.
34. Chopra, N., Mansingh, A. and Chadha, G., "Electrical, optical and structural properties of amorphous V_2Os-TeO_2 blown films". J. Non-Cryst. Solids., 1990, 126, 194-201.
35. Turky, G. and Dawy, M., "Spectral and electrical properties of ternary (TeO_2–V_2O_5–Sm_2O_3) glasses". Mater. Chem. Phys., 2003, 77, 48-59.
36. Souri, D. and Salehizadeh, S. A., "Effect of NiO content on the Optical band gap, refractive index and density of TeO_2-V_2O_5-NiO glasses". J. Mater. Sci., 2009, 44, 5800-5805.
37. Swanepoel, R., "Determination of the thickness and optical constants of amorphous silicon". Physics E., 1983,16, 1214-1222.
38. Ahmad A.A., Alsaad A.M., Albiss B.A., Al-Akhras M.A., El-Nasser H.M. and Qattan I.A., "The effect of substrate temperature on structural and optical properties of DC sputtered ZnO thin films". Physica B: Condens Matter., 2015, 470, 21-32.
39. Rakhshani A., "Study of Urbach tail, bandgap energy and grain-boundary characteristics in CdS by modulated photocurrent spectroscopy".

[DOI: 10.22068/ijmse.15.3.21]

J. Phys.: Condens. Matter., 2000,12, 4391-4400.
40. Tauc J., "Amorphous and liquid semiconductors". Springer Science & Business Media., 2012.
41. Poelman D. and Smet P.F., "Methods for the determination of the optical constants of thin films from single transmission measurements: a critical review". J. Phys. D: Appl. Phys., 2003, 36, 1850.
42. Ehsani, M. H., Zarei Moghadam, R., Rezagholipour Dizaji, H., and Kameli, P., "Surface modification of ZnS films by applying an external magnetic field in vacuum chamber". Mater. Res. Express., 2017, 4, 096408.
43. Tajik, N., Ehsani, M. H., Moghadam, R. Z. and Dizaji, H. R., "Effect of GLAD technique on optical properties of ZnS multilayer antireflection coatings". Mater Res Bull., 2017, 100, 265-274.
44. El-Shazly, A. and El-Shair, H., "Some parameters affecting the optical constants of CdTe thin evaporated films". Thin Solid Films., 1981, 78, 287-293.
45. Dejpasand, M. T., Ehsani, M. H., and Rezagholipour, Dizaji, H., "Substrate temperature effect on the structural, morphological and optical properties of CdTe films". MATER RES INNOV., 2016, 1-8.
46. Ebnalwaled, A., Yousef, A., Gerges, M. and Thabet, A., "SYNTHESIS OF NANO-POLYIMIDE FOR MICROELECTRONIC APPLICATIONS". J. Applied. Chem. Sci., 2016, 6, 18-30.
47. Al-Mudhaffer, M. F., Nattiq, M. A. and Jaber, M. A., "Linear optical properties and energy loss function of Novolac: epoxy blend film". Appl. Sci. Res., 2012, 4, 1731-7140.
48. Murugan, R., Vijayaprasath, G. and Ravi, G., "The influence of substrate temperature on the optical and micro structural properties of cerium oxide thin films deposited by RF sputtering". Superlattices Microstruct., 2015, 85, 321-330.

[DOI: 10.22068/ijmse.15.3.21]